Ceramics International 46 (2020) 5876–5886

Contents lists available at ScienceDirect

Ceramics International

journal homepage: www.elsevier.com/locate/ceramint

New observations on wear characteristics of solid Al_2O_3/Si_3N_4 ceramic tool in high speed milling of additive manufactured Ti6Al4V

Jiaqiang Dang[a,b], Heng Zhang[a,b], Weiwei Ming[a,b,*], Qinglong An[a,b], Ming Chen[a,b]

[a] State Key Laboratory of Mechanical Systems and Vibration, Shanghai Jiao Tong University, Shanghai, 200240, China
[b] School of Mechanical Engineering, Shanghai Jiao Tong University, Shanghai, 200240, China

ARTICLE INFO

Keywords:
Additive manufacturing
Ti6Al4V
High-speed milling
Solid ceramic tool
Wear behavior

ABSTRACT

Additive Manufacturing (AM) technologies applied to the titanium alloys have attracted attention from industries in recent years. Despite one of the main goals of AM is the reduction of manufacturing steps, semi-finish/finish machining operations are still required so as to obtain the desired geometrical tolerance and surface features. In this study, the solid end mill was manufactured by Al_2O_3/Si_3N_4 (Sialon) ceramic materials and employed in high-speed slot milling of Ti6Al4V alloy fabricated by the Direct Metal Laser Sintering (DMLS) AM technology to study the tool wear characteristics during processing. The Raman spectroscopic method was employed to characterize the molecular structures of Sialon ceramics for the manufacturing of the cutting tool. The morphologies and elemental maps of wear region of the ceramic tool were examined by scanning electron microscope and energy dispersive spectroscopy techniques. The results show that the adhesion wear and diffusion wear are the dominant wear mechanisms, and the chemical stability of Al_2O_3/Si_3N_4 (Sialon) ceramics fabricated as the solid ceramic tool to the attack of the atoms from additive manufactured Ti6Al4V is relatively weak under the atmosphere. The difference of thermal expansion coefficients of diffusion layer and tool substrate accelerates the initiation and propagation of thermal cracks formed on the diffusion interface. Moreover, fracturing and crater-like groves near the tool edge were finally formed due to the removal of adhered workpiece material.

1. Introduction

Ti6Al4V alloy, namely TC4 or Ti64, has nowadays received considerable interest in many industries thanks to their unique metallurgical and physical properties. To be specific, Ti6Al4V is an $\alpha+\beta$ alloy with advantages of high specific hot strength, excellent corrosion and fracture resistance and well-documented biocompatibility [1]. Characterized as the most common titanium alloy, it was used for the production of almost half of titanium products employed worldwide today [2]. Ti6Al4V alloy was firstly utilized for the production of aerospace components and then extended to biomedical parts, such as jet engines, airframe components, acetabular cups and knee joints [3–7]. As a matter of fact, components of the aerospace and biomedical fields usually present complex shapes that require time-consuming manufacturing chains for their production. Conventional methods are involved in forging and casting of bulk materials, followed by machining operations to final required dimensions and shapes. However, the aforementioned machining processes often lead to significant material waste [8].

In recent years, additive manufacturing (AM) commonly known as 3D printing, has been applied for *near-net-shape* products with geometric complexities using computer-aided design (CAD) models, being easier and faster than conventional processes [8–10]. Compared to conventional manufacturing processes of Ti6Al4V products, the great superiority of AM lies in its flexibility and designability by reducing the conventional process chains such as hot forming at high temperatures, extrusion and rough machining operations. These advantages greatly cut down the expenses since the material cost and manufacturing cost are significantly reduced [8,11–13]. And the method of Direct Metal Laser Sintering (DMLS) has been increasingly adopted by manufacturers in AM processes because of the advantage of high localized heat input in a very short interaction time [14,15]. While the AM parts show randomly dispersed defects and microstructural heterogeneities, as well as different mechanical characteristics compared to those manufactured by conventional processes. Despite that AM can reduce the manufacturing steps, finishing operations are still required to satisfy the joining features and obtain the high geometrical tolerances [16].

The processing of titanium alloys, including Ti6Al4V alloy

* Corresponding author. State Key Laboratory of Mechanical Systems and Vibration, Shanghai Jiao Tong University, Shanghai, 200240, China.
E-mail address: mingseas@sjtu.edu.cn (W. Ming).

https://doi.org/10.1016/j.ceramint.2019.11.039
Received 26 October 2019; Received in revised form 1 November 2019; Accepted 5 November 2019
Available online 06 November 2019
0272-8842/

manufactured by additive manufacturing and forging methods, has been challenging owing to their high strength at elevated temperatures and poor thermal conductivity [17–19]. The difficulty of heat dissipation in the cutting process leads to high cutting temperatures concentrated in the narrow region adjacent to the cutting edge [20]. In some cases, the temperature can reach over 1000 °C in the cutting zone [21]. Several tools have been used to machine titanium alloys, such as coated and uncoated cemented carbides, and superhard tools [22–25]. However, the signs of wear of the mentioned cutting tools are serious since another significant characteristic of additive manufactured Ti6Al4V is its active chemical reactivity with most cutting tool material in the atmosphere [26,27]. To ensure machining efficiency, one of the efficient ways is hunting for new cutting tools with excellent mechanical properties at elevated temperatures. At aggressive cutting conditions, ceramics the Al_2O_3/Si_3N_4 (Sialon) in particular, show great advantages during machining hard materials owing to the superior thermo-mechanical properties over cemented carbide tools [28–31].

Even if the ceramic tools in the form of indexable inserts have been studied and applied in high-speed cutting of hard materials [32–34], there are limited publications concerning the application of solid ceramic tools in the high-speed milling process. The main reason can be attributed to the severe fracture of the cutting edge of the cutting tool during the milling process. Wang et al. [35] examined the cutting performance of solid ceramic tools during machining of AISI H13 steel and reported that the performance of solid ceramic milling tools outperformed WC-Co based milling tools. In recent work, Celik et al. [36] used solid Sialon milling tools to investigate the wear behavior during high-speed milling of Inconel 718 and found that the dominant wear mechanism was the diffusion-based wear of the tools. However, from the literature survey, note that investigations on the high-speed machining of additive manufactured Ti6Al4V with solid Sialon milling tools concerning tool wear mechanism and mechanical issues are rare. Therefore, the massive adoption of Sialon tools by industries is slowed down due to a lack of relevant knowledge.

For this purpose, the present work aims to reveal the wear mechanisms of solid Al_2O_3/Si_3N_4 based ceramic cutter during dry high-speed milling of additive manufactured Ti6Al4V alloy. Solid Sialon ceramic cutter was tested on the slot milling tests at high cutting speeds, up to 250 m/min and tool wear characteristics were investigated. Worn surfaces of the solid ceramic tool after milling tests were measured by scanning electron microscope (SEM) and energy dispersive spectroscopy (EDS) techniques.

2. Experimental procedures

2.1. Characterization of the workpiece material

The Ti6Al4V specimen under investigation was produced by Direct Metal Laser Sintering (DMLS) AM technique. To be specific, the researched cuboid Ti6Al4V samples were printed by an EOS™ EOSINT M280 machine with a laser power of 2–3 kW and a spot diameter of 3 mm. In the AM process, a molten pool where rapid melting and resolidification take place was generated. A typical martensitic microstructure with needle-like morphology was produced after the printing process since there is no pre-heating for the used material and the cooling rate during the processing is relatively high. The raw DMLS parts have limited applications since they are associated with high residual stress and excessive-high hardness. Therefore, heat treatment is necessary for the DMLS raw specimen so as to the subsequent machining and final production. In this work, the studied workpiece material was heat-treated DMLS Ti6Al4V titanium alloy. The working principle of the DMLS process and the used machining specimen of heat-treated DMLS Ti6Al4V alloy are illustrated in Fig. 1(a) and (b), respectively. Before the slot milling tests, the samples in section A obtained from the additive manufactured Ti6Al4V were embedded into the hot mounted resin, then ground and polished, and finally etched with the Kroll's reagent. The microstructure of the additive manufactured Ti6Al4V titanium alloy obtained by scanning electron microscope (SEM) is shown in Fig. 1(c). It can be noted that a columnar microstructure of the α phase with intergranular β phase is characterized in the SEM micrograph. There is a distinct boundary between α and β phases: the dark region is the α phase while the light region is the β phase. Besides, the chemical compositions (*wt.* %) of the AM Ti6AL4V samples according to the EDS analysis are shown in Table 1.

2.2. Details of solid Al_2O_3/Si_3N_4 ceramic cutting tool

The commercial solid Al_2O_3/Si_3N_4 ceramic end mill used in the machining tests of the present work is also known as Sialon based ceramic tool, which was supplied by the OSG company. The external shape dimensions of the end mill are summarized as follows: the diameter of 8 mm, corner radius of 1 mm, blade length of 6 mm, the whole length of 60 mm and 4 flutes. The tip and side views, as well as the external shape dimensions of the used Sialon ceramic tool, are plotted in Fig. 2. The Sialon based ceramic tool material is mainly composed of Si_3N_4, Al_2O_3 and Y_2O_3. The aim of sintering additives is to promote the densification of raw ceramic powders during the fabrication process. The ceramic bar was firstly fabricated by hot pressing technology and at last the four-edge milling tool with the final dimensions was obtained through grinding. The physical and mechanical properties of the ceramic tool material were obtained from the cutting tool supplier, which are summarized in Table 2. The excellent properties of high oxidation resistance and high thermal conductivity make it suitable for high-speed cutting operations of difficult-to-machine materials with dry condition.

Meanwhile, the Raman spectroscopic method was employed to characterize the molecular structures of Sialon ceramics for the manufacturing of the cutting tool. The Raman image was extracted from the flank face of the reported Sialon tool using an Invia Qontor instrument equipped with confocal Raman. This device has a spectral resolution of 1.0 cm^{-1} and the range of 4500 cm^{-1} to 80 cm^{-1}. The Raman spectrum in the current work was observed by the excitation using a laser wavelength of 532 nm. After the running process, the obtained data were processed and the background level was then removed by the corresponding software of WiRE 5.1. Fig. 3(a) and (b) show the complete results of Raman image extracted from tool flank face and Raman spectrum of the tested Al_2O_3/Si_3N_4 composite on the tool flank face, respectively.

It can be noted that the Raman spectrum in Fig. 3(b) resembles that of β-Si_3N_4 reported by Takase et al. [37–39]. However, the entire bands of our results shift to lower frequency by about 7 cm^{-1} compared to the previous study [40]. This phenomenon can be attributed to the increase of Al_2O_3 content during the fabrication process of the cutting tool in this work. It is known that Si and N of the β-Si_3N_4 are replaced by Al and O of Al_2O_3 during the fabrication of Sialon. An increase of the Al_2O_3 content will lead to an elevation of structural disorder for the β-Si_3N_4. This will, therefore, result in a decrease in the long-range order for the periodic lattice structure since the Raman bands below 300 cm^{-1} are assigned to lattice vibrational modes [39]. The first four intense bands at 178 cm^{-1} (L_1), 198 cm^{-1} (L_2), 222 cm^{-1} (L_3) and 255 cm^{-1} (L_4) may be ascribed to lattice modes since Raman bands generally due to lattice modes are stronger than those of internal modes [38]. The other bands between 300 $cm^{-1}$and 1200 cm^{-1} are assigned to internal modes, especially attributed to the stretching vibrational modes of Si–N above 800 cm^{-1} and the bending modes of Si–N–Si and N–Si–N between 750 cm^{-1} and 400 cm^{-1} [37].

2.3. Machining tests

All the dry slot milling tests were performed on a vertical machining center (HURCO VMAX 42) with a maximum spindle speed of 12000 rpm. The schematic diagram and the arrangement of the

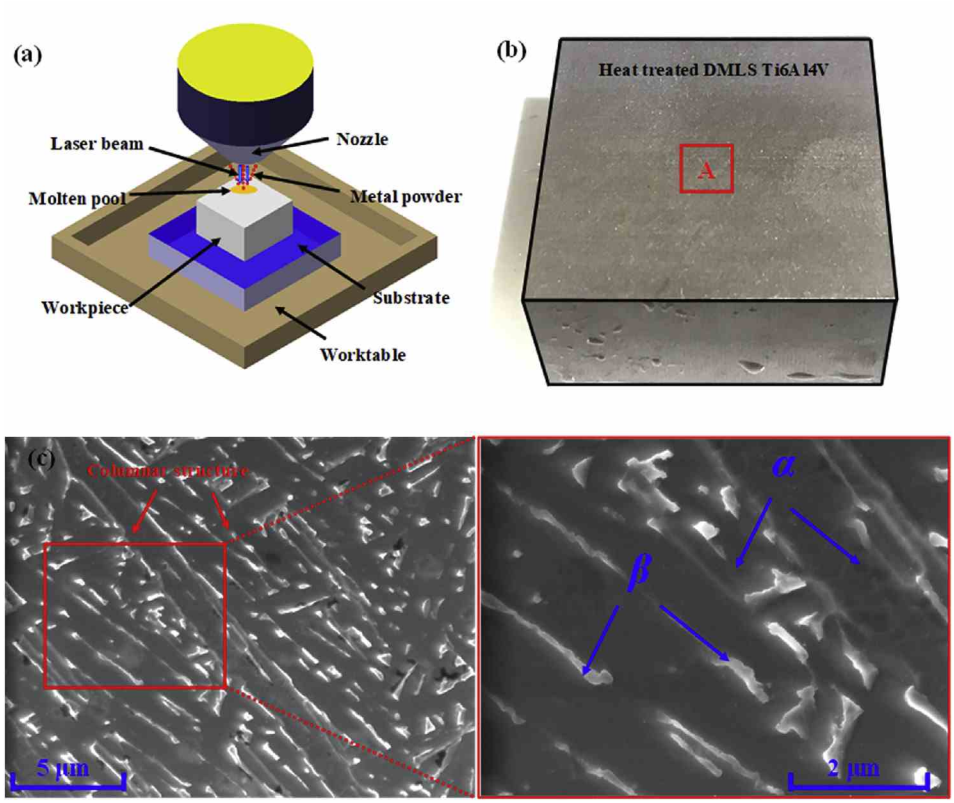

Fig. 1. (a) Working principle of DMLS process; (b) Heat-treated DMLS Ti6Al4V specimen; (c) SEM micrograph of the additive manufactured Ti6Al4V alloy.

Table 1
Chemical compositions of additive manufactured Ti6Al4V according to EDS.

Element	Ti	N	O	Na	Al	Cl	K	C	V	M
wt.%	Bal.	0.36	0.04	0.22	5.79	0.34	0.23	0.81	4.49	0.94

experimental setup for high-speed slot milling tests are present in Fig. 4(a) and (b), respectively. The cutting experiments involved in AM Ti6Al4V titanium alloy workpiece, solid Sialon based ceramic tool, fixture and signal capture devices including cutting forces and temperature field. The specimen with an external size of 50 mm × 50 mm × 50 mm was firmly clamped onto a piezoelectric dynamometer (Kistler 9272) in connection with a multichannel charge amplifier (Kistler 5070A). The *in-situ* force signals characterized as main cutting force (*Fx*), feed force (*Fy*) and thrust force (*Fz*) during the slot milling process were carefully recorded. Besides, the cutting temperature field was captured by an infrared thermal imager (FLIR A615) which has a spatial resolution of 0.68 mrad and a calibrated temperature range of 20-2000 °C. All the force and temperature data can be exported and analyzed by the corresponding software installed on a personal computer. The processing parameters of cutting speed were 250 m/min with a feed rate of 0.05 mm/tooth and axial depth of cut of 0.5 mm. It should be noted that the cutting parameters utilized in this paper are selected according to the parametric range for solid Sialon ceramic end mill recommended by the tool manufacturer. The experiments were performed without using any cutting fluids and coolants since the ceramic materials have excellent high-temperature resistance.

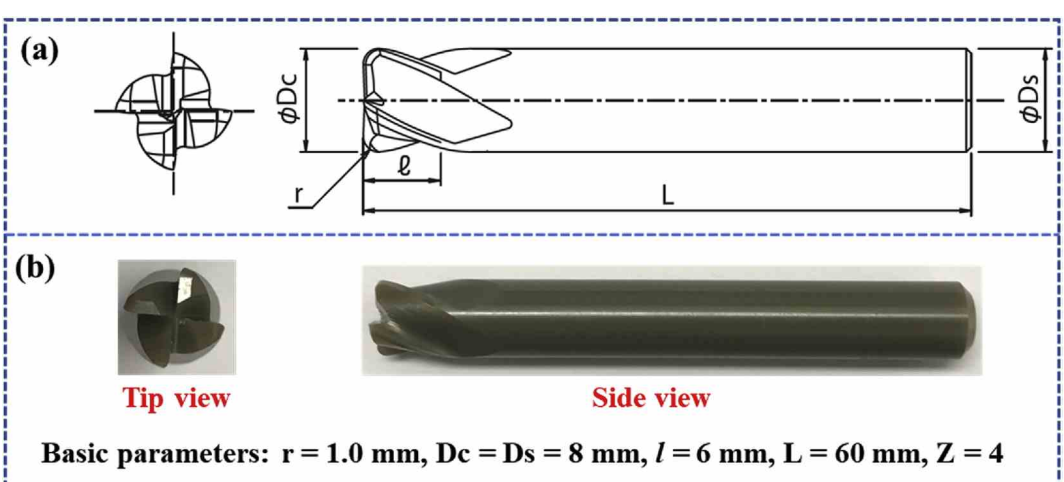

Fig. 2. (a) External shape dimensions and (b) images and basic parameters of the solid ceramic end mill.

Table 2
Physical and mechanical properties of the Sialon based ceramic tool material.

Sample	Main tool material			Flexural strength (MPa)	Fracture toughness ($MPa·m^{1/2}$)	Bending strength (MPa)	Density (g/cm^3)
Sialon	Al_2O_3	Si_3N_4	Y_2O_3	1200	4.45	950	3.2

During the slot milling process, each cycle was stopped when the side length of the workpiece was machined. There are totally 16 progressive cycles carried out for the ceramic tool and the whole cutting length was measured as 800 mm. In the slot milling process, the material removal rate was calculated as up to 7957.6 mm^3/min according to the employed cutting variables. This paper mainly aims to address the tool wear characteristics of solid Sialon ceramic tool when dry high-speed milling of AM Ti6Al4V alloy while the analysis of other cutting responses such as cutting forces and machined surface integrity is out of the scope of this paper, which will be discussed in the future work. At the end of the cutting tests, the worn tool was inspected by SEM (MIRA3 TESCAN) and EDS (Aztec X-MaxN 80) to determine the dominant wear mechanism and failure modes of the researched Sialon tool.

3. Results and discussion

3.1. Morphology evolution of tool rake and flank faces

During the slot milling experiments, the tool morphology with respect to the machining distance was carefully detected to figure out how the tool wear evolved during the processing. Fig. 5 gives the SEM micrographs of tool rake and flank faces of the solid Sialon ceramic tool after undertaking a cutting distance of 0, 500 and 800 mm. It can be noted that the adopted cutting tool was exposed to significant mechanical and thermal loads during the machining process. The tool rake and flank faces were both encountered with the material that to be machined and the interface temperature at the cutting zone was relatively high concerning the wear signs of the tool. Before the machining tests, the solid ceramic tool showed smooth surfaces and a sharp edge, which indicated the superior cutting performance of the tool. However, the tool surfaces became rough and chipping appeared on the tool edge after finishing a cutting distance of 500 mm for the Sialon tool. As the cutting process continued to progress, the deformation of tool edge occurred and the adhesion of workpiece was increasingly serious. Furthermore, some craters along the tool flank surface were also formed. The final tool morphologies observed from the tool rake face and flank face after completing the cutting distance of 800 mm for the solid ceramic tool were plotted in Fig. 5(c) and (f), respectively.

Fig. 6 plots the SE – SEM images of sections A, B, C and D in Fig. 5 with higher magnification for better characterization of the solid Sialon tool morphologies after the arranged slot milling tests. It can be seen that both the rake face and flank face of the tool was covered by the AM Ti6Al4V during the machining experiments. This phenomenon also indicates that a high strain rate of the machined material and high cutting temperatures were induced due to the high cutting speeds employed in the processing. It was reported by Gu et al. [41] that the temperature evidently decreases from the shear band zone to the chips, being about 200-500 °C during high-speed machining of the Ti6Al4V titanium alloy while the highest temperature reaches up to 1300 °C in the first heating zone. According to Zheng et al. [42], based on high-speed turning of Inconel 718 with Sialon-Si_3N_4 ceramic tool, they concluded that the high cutting temperatures are the reason for the severe adhesion of workpiece material on the cutting tool faces. Furthermore, the study by Tian et al. [43], after high-speed face milling of Inconel 718 with Sialon tools, showed that the adhesion based wear was the main wear behavior when the adopted cutting speeds exceed 1400 m/min. In this work, the solid Sialon ceramic tool was tentatively used to slot mill the additive manufactured Ti6Al4V alloy with the aim of figuring out the machining-induced wear behavior of the tool. In Fig. 6(a) and (c), the rake face and flank face of the fresh tool were shown, being maintained at a smooth level and the grinding marks remained during manufacturing of the tool can be clearly observed. Considering the mechanical and thermal properties associated with AM Ti6Al4V, severe adhesion of the workpiece was expected to form on the tool faces during the processing. After finishing 800 mm slot milling tests, SE- and BSE-SEM techniques were introduced to measure wear morphologies of the tool faces. It was shown that characteristic adhesion traces with massive and platy structures on the tool rake face and flank face were captured by SE – SEM, as shown in Fig. 6(b) and (d), respectively. Fig. 7 shows the BSE-SEM images of tool faces after all the tests, in which the mass thickness contrast revealing the obvious chip welding phenomenon was illustrated. This behavior agrees well with the peculiar machinability of additive manufactured Ti6Al4V alloy

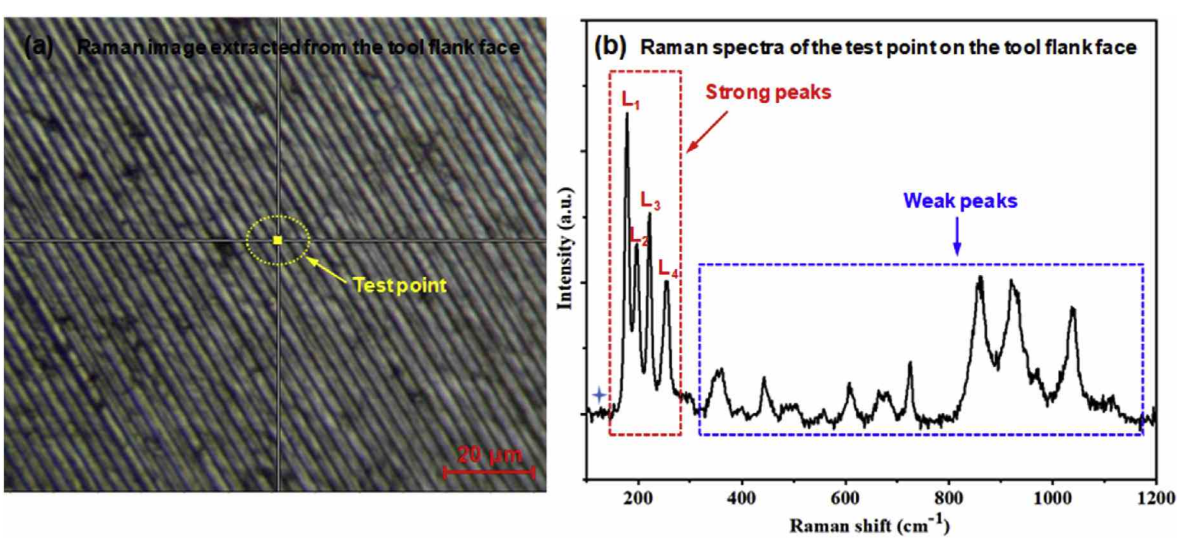

Fig. 3. Results of Raman image and spectra of the reported Al_2O_3/Si_3N_4 composite.

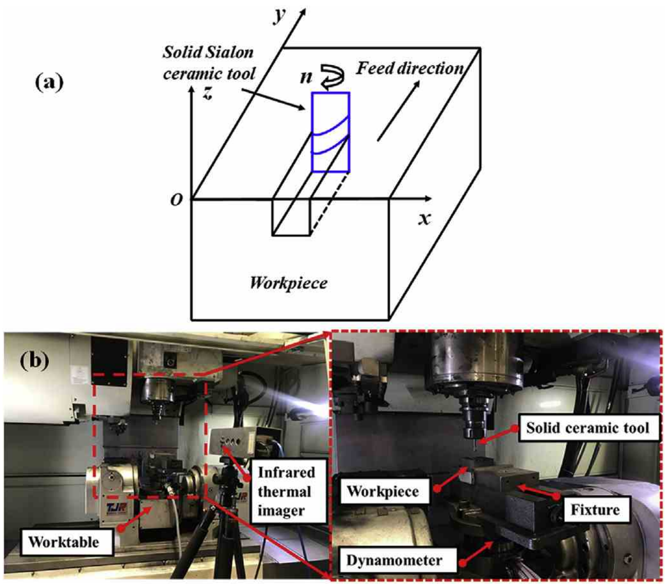

Fig. 4. (a) Schematic diagram and (b) experimental setup for high-speed milling tests.

during the cutting process, which has been mentioned before.

3.2. Tool wear modes

The wear modes of solid Sialon ceramic tool during high-speed machining of additive manufactured Ti6Al4V were characterized by the analysis of the element diagram of the worn tool. Fig. 8 presents the SEM images of wear morphology and EDS results of elemental distribution maps taken from the tool rake face after all the cutting tests. From the wear morphology in Fig. 8(a), it can be seen that the wear of the tool was mainly concentrated upon the vicinity of the tool edge corner since the axial cutting depth arranged in the present work is small. The main objective of this paper lies in the exploration of macroscopically cutting performance of the solid ceramic tool and the wear mechanisms for the adopted Sialon ceramic tool are the core content of this manuscript. Therefore, representative parts of worn surfaces with higher magnification are also shown in this figure, as observed in Fig. 8(b) and (c). It can be seen from the image of Fig. 8(a) that plastic deformation appears on the cutting edge and severe wear occurs on the rake face of solid Sialon ceramic tool, especially for the vicinity of the tool edge corner. This behavior can be attributed to the high thermal and mechanical loading in view of the poor machinability of the workpiece material. On the other hand, intermittent cutting leads to severe impact which repeatedly acts on the tool edge during the milling process. The SEM micrograph with higher magnification in Fig. 8(b) indicates that there is carbide and diffusion trace spreading over the tool rake face closed to the zone of tool edge corner. The removal of tool substrate material will happen when the external load exceeds the bonding strength of diffusion layer, the mechanism of which will be detailedly discussed based on the elemental analysis in later sections. The chipping of tool edge was also observed, as shown in Fig. 8(c), which mainly attributes to the thermal and mechanical impacts during the slot milling process. The EDS results in Fig. 8(d) and (e) showing the elemental maps of detected points from the tool rake face agree well with the wear analysis as mentioned before.

Fig. 9 presents the SEM images of wear morphology and EDS results of elemental distribution maps taken from the tool flank face after finishing all the milling tests. It can be indicated from Fig. 9(a) that there are severe abrasion and crater appeared on the vicinity zone of tool edge while the residual adhered workpiece was evidently observed on the tool flank face. During the slot milling process of additive manufactured Ti6Al4V, the cutting edges of the ceramic tool undertook much high cutting temperature being recorded as higher than 1200 °C (Please see the screenshot of temperature field and the temperature evolution of region A during the stead milling process in Fig. 10(a) and (b), respectively). Although an increase of the temperature has little influence on the cutting performance of the ceramic tool, severe adhesion and subsequent diffusion of the workpiece material were expected to form on the tool surface during the processing. With respect to the diffusion layer of the workpiece into the tool substrate, thermal

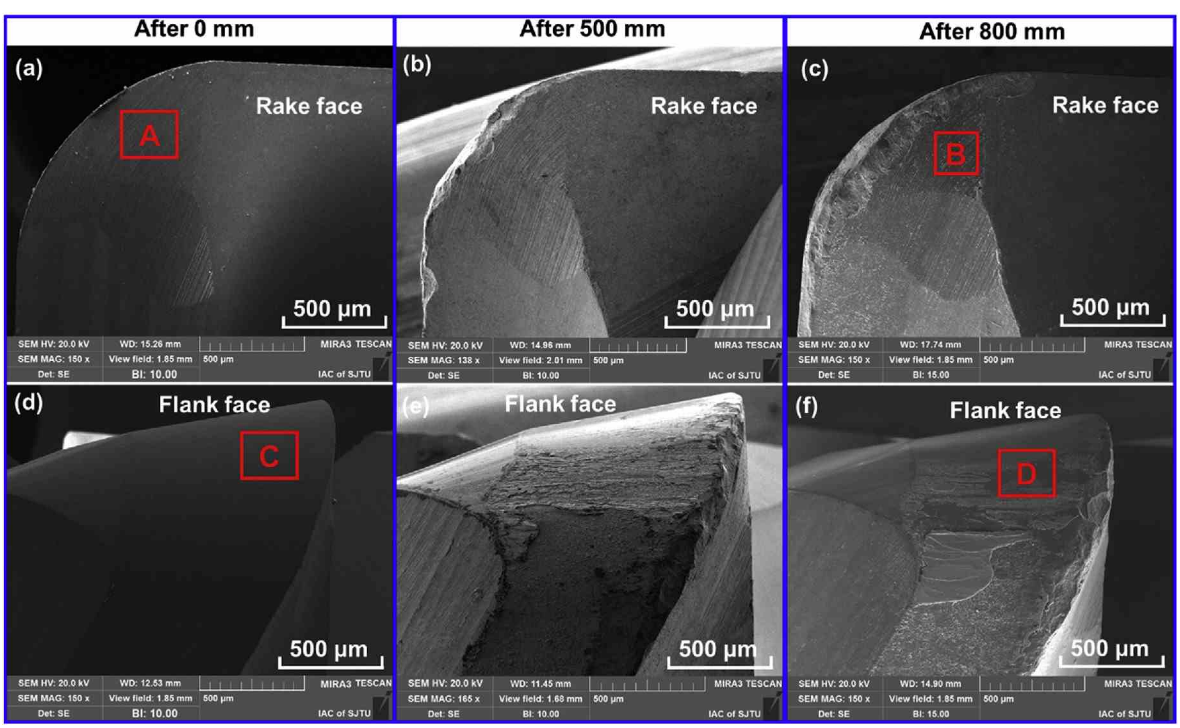

Fig. 5. SEM micrographs of the tool rake face and flank face after 0, 500 and 800 mm slot milling tests.